



## Phonon dynamics of the Sn/Ge(1 1 1)-(3 × 3) surface

D. Farías<sup>a,\*</sup>, W. Kamiński<sup>b,c</sup>, J. Lobo<sup>a</sup>, J. Ortega<sup>b</sup>, E. Hulpke<sup>d</sup>, R. Pérez<sup>b</sup>,  
F. Flores<sup>b</sup>, E.G. Michel<sup>a</sup>

<sup>a</sup>Departamento de Física de la Materia Condensada and Instituto Nicolás Cabrera, Universidad Autónoma, 28049 Madrid, Spain

<sup>b</sup>Departamento de Física Teórica de la Materia Condensada, Universidad Autónoma, 28049 Madrid, Spain

<sup>c</sup>Institute of Experimental Physics, University of Wrocław, pl. Maska Borna 9, 50-204 Wrocław, Poland

<sup>d</sup>Max-Planck-Institut für Strömungsforschung, Bunsenstr. 10, 37073 Göttingen, Germany

Available online 4 August 2004

### Abstract

We present a theoretical and experimental study on the phonon dynamics of the low-temperature Sn/Ge(1 1 1)-(3 × 3) structure. High-resolution helium atom scattering (HAS) data show that, besides the Rayleigh wave, there are three surface phonon branches with low dispersion related to the (3 × 3) surface phase. Their energies are approximately 6.5, 4, and 3 meV at the  $\bar{\Gamma}$  point. In addition, we detect phonon peaks in the  $Q$  range 0.4–0.5  $\text{\AA}^{-1}$  at ~2 meV, which correspond to (3 × 3) folding of the Rayleigh wave. Ab initio DFT–GGA total energy calculations have been performed to determine the frequencies associated with the vertical displacements of the three Sn atoms in the unit cell. The values obtained are in good agreement with the experiment.

© 2004 Elsevier B.V. All rights reserved.

PACS: 68.35.Ja; 73.20-r; 68.35.Rh; 71.15.Nc; 71.15.Ap

Keywords: Phase transitions and critical phenomena; Surface and interface dynamics and vibrations; Phonons-low-dimensional structures; DFT–GGA; Phonon

### 1. Introduction

Phase transitions in low-dimensional systems provide insight into several fundamental aspects of solid state physics, and have therefore been extensively investigated in the past [1,2]. The system formed by 1/3 of a monolayer (ML) of Sn in Ge(1 1 1) undergoes

a temperature-induced phase transition between room temperature (RT) and low temperature (LT). This phase transition presents a complex experimental behavior that has given rise to several controversial interpretations on its physical properties [3–14]. This fact and the accessible temperature range explain the considerable attention received in recent years [3–14]. The RT surface structure corresponds to a  $(\sqrt{3} \times \sqrt{3})R30^\circ$  superperiodicity. It reverts to a (3 × 3) at LT [3]. In both phases Sn adatoms occupy the  $T_4$  coordination sites of the unreconstructed Ge(1 1 1)

\* Corresponding author. Tel.: +34-91-497-5550;  
fax: +34 91 397 39 61.

E-mail address: [daniel.farias@uam.es](mailto:daniel.farias@uam.es) (D. Farías).

substrate [5,6]. All Sn adatoms look similar in the  $(\sqrt{3} \times \sqrt{3})R30^\circ$  phase when observed with scanning tunneling microscopy (STM) [3]. As the  $(3 \times 3)$  phase is stabilized at LT, a  $(3 \times 3)$  asymmetry shows up in the STM images. Surface X-ray diffraction experiments have concluded that this asymmetry is due to a total vertical distortion of  $\sim 0.3 \text{ \AA}$  between the three adatoms that form the unit cell (one is displaced upwards and the other two inwards), both for Sn/Ge(1 1 1)<sup>5</sup> and Pb/Ge(1 1 1)<sup>6</sup>. Different models have been put forward to explain the structural and electronic properties of the phase transition [3–14]. In the dynamical fluctuations model [4], Sn adatoms fluctuate at RT between ‘up’ and ‘down’ positions, with a correlated motion that keeps locally the  $(3 \times 3)$  structure, explaining the apparent contradiction between electronic and structural evidences [3,4,9]. STM studies have shown that defects have a significant influence on the phase transition [10,11], stabilizing  $(3 \times 3)$ -ordered regions around them. Recent theoretical work has proposed that a soft phonon associated with the dynamical fluctuations of the Sn atoms may be the driving force of this phase transition [15]. This prediction has been recently confirmed by experiments which demonstrate the existence of a phonon softening in the RT phase [16]. Theoretical calculations relate the surface phonon associated with the vertical fluctuation to the  $(3 \times 3)$  ordering around defect sites [12].

In this work, we report a combined experimental and theoretical study on the phonon dynamics of the  $(3 \times 3)$  structure. The experimental dispersion curves were determined using high-resolution helium atom scattering (HAS), and show the existence of three low-dispersion bands in addition to a Rayleigh wave. Also, several points were found in the  $Q$  range  $0.4\text{--}0.5 \text{ \AA}^{-1}$  at  $\sim 2 \text{ meV}$ , which correspond to the  $(3 \times 3)$  folding of the Rayleigh wave, as expected for the existence of a well-ordered  $(3 \times 3)$  structure. Understanding this complicated phonon spectrum has required a combination of ab initio DFT–GGA total energy calculations and numerical fitting of an up to second-nearest-neighbor force constant model to the experimental data. This combined approach allows us to identify the character of the different modes in terms of the  $z$ -displacements of the three Sn atoms in the unit cell and to predict phonon frequencies in excellent agreement with the experimental results.

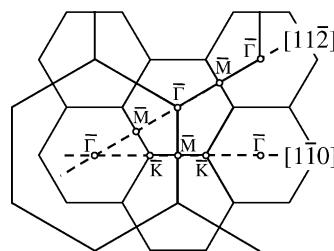


Fig. 1. Reciprocal space of the  $(\sqrt{3} \times \sqrt{3})R30^\circ$  (bold lines) and  $(3 \times 3)$  (thin lines) structures. High symmetry crystallographic directions are shown as dashed lines. The lettering refers to the symmetry points of the  $(3 \times 3)$  structure.

## 2. Experimental

The experiments were performed in a high-resolution helium atom scattering (HAS) time-of-flight (TOF) apparatus that has been described previously [16,17]. The Ge(1 1 1) crystal was cut from a n-type polished commercial wafer ( $\pm 0.5^\circ$ ,  $\rho < 0.4 \text{ \Omega cm}$ ). The surface temperature was monitored using a thermocouple situated very close to the sample. The sample temperature during the experiments was 140 K, well below the critical temperature of the phase transition [16]. The sample was prepared following the same procedures described in references [4,6,18].

Coverage was calibrated by monitoring the intensity of a  $1/3$  peak along the  $[1\bar{1}0]$  azimuth (see Fig. 1), which exhibits a maximum at a coverage of  $1/3 \text{ ML}$  (see Fig. 2). We used a low deposition rate ( $1 \text{ ML/}$

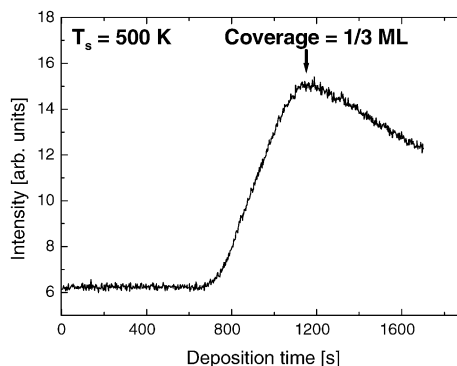


Fig. 2. Evolution of the  $(1/3, 1/3)$  peak along  $[1\bar{1}0]$  as a function of Sn deposition time. The sample temperature was 500 K, and the deposition rate  $1 \text{ ML/60 min}$ .

60 min) that allows to determine the ideal coverage of 1/3 ML within  $\pm 0.01$  ML [19] (1 ML is defined as the Ge(1 1 1) surface density,  $7.21 \times 10^{14}$  atoms/cm<sup>2</sup>).

### 3. Results and discussion

Fig. 3 shows HAS angular distributions of the  $(3 \times 3)$  phase recorded along the two high symmetry directions ( $[1\ 1\ \bar{2}]$  and  $[1\ \bar{1}\ 0]$ , see Fig. 1). The sharp diffraction peaks indicate that the reconstruction is of high quality. The full width at half maximum (FWHM) of the fractional order peaks is  $\sim 0.25^\circ$ . From this value, the average domain size can be estimated in  $\sim 200$  Å [20]. The incidence conditions were chosen in such way that the specular intensity was maximum, since phonon measurements are performed at angles of incidence close to the specular one. For the Sn/Ge(1 1 1)- $(3 \times 3)$  surface this corresponds to a beam temperature of 138 K, i.e. to  $k_i = 7.54$  Å<sup>-1</sup> and  $E_i =$

29.7 meV. From the relative intensity between the specular and the fractional order peaks we conclude that the corrugation amplitude of the  $(3 \times 3)$  phase is not very large, i.e. not larger than  $\sim 0.3$  Å.

Time-of-flight spectra were recorded along the two main symmetry directions to probe the low-energy dynamical vibrations of the  $(3 \times 3)$  phase. Different momentum transfers have been sampled by changing the incidence angle and the incident He beam energy. Typically, incidence angles  $\theta_i$  ranged from  $47^\circ$  to  $53^\circ$ , and the incident beam energies from  $E_i = 20$  to 30 meV. Representative TOF spectra recorded at  $E_i = 23.8$  meV ( $k_i = 6.75$  Å<sup>-1</sup>) are shown in Fig. 4. The largest peak located at  $\sim 2100$  μs corresponds to the diffuse quasielastic peak, and additional peaks corresponding to single phonon events are clearly resolved. The diffuse quasielastic peak is much more intense than any other peak by roughly a factor of 5. This suggests the existence of surface defects in the  $(3 \times 3)$  phase, in agreement with STM findings [10]. Indeed, HAS is very sensitive to the presence of surface defects. Their density can be estimated from the spectra shown [17] as  $< 5\%$ , also in agreement with STM results [10].

Since the formation of the  $(3 \times 3)$  structure affects more strongly the  $[1\ 1\ \bar{2}]$  direction (see Figs. 1 and 3), we concentrate in the following on the data corresponding to this direction. Fig. 5 shows the phonon dispersion curves along  $[1\ 1\ \bar{2}]$  obtained by converting the TOF-data into energy loss spectra. A comparison with the phonon modes of the clean Ge(1 1 1)-c $(2 \times 8)$  surface [21] allows to identify the mode at lower energies with  $Q = 0.0\text{--}0.2$  Å<sup>-1</sup> as the Rayleigh wave. As it is expected for a well-ordered surface reconstruction where the atoms exhibit well-defined vibrational modes, the Rayleigh wave is folded in the new  $(3 \times 3)$  unit cell. The points found in the  $Q$  range  $0.4\text{--}0.5$  Å<sup>-1</sup> at  $\sim 2$  meV are due to this folding. An estimate of the Rayleigh wave dispersion, folded into the  $(3 \times 3)$  unit cell, is shown as dashed lines in Fig. 5. Additional experimental points in Fig. 5 are typical of the  $(3 \times 3)$  phase. They are within the gap of the projected bulk phonon modes. Thus, we conclude that these points can be identified as coming from surface phonon modes. We detect a branch with low dispersion around 6.5 meV, and two additional modes around 4 and 3 meV.

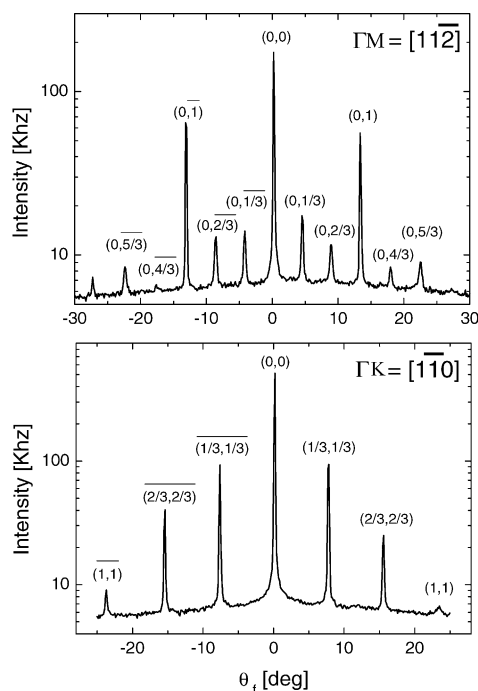


Fig. 3. HAS angular distributions recorded from the  $(3 \times 3)$  phase along the  $[1\ 1\ \bar{2}]$  (top) and  $[1\ \bar{1}\ 0]$  (bottom) azimuths. The surface temperature is 140 K. The incoming He beam wave vector is  $7.54$  Å<sup>-1</sup> ( $E_i = 29.7$  meV).

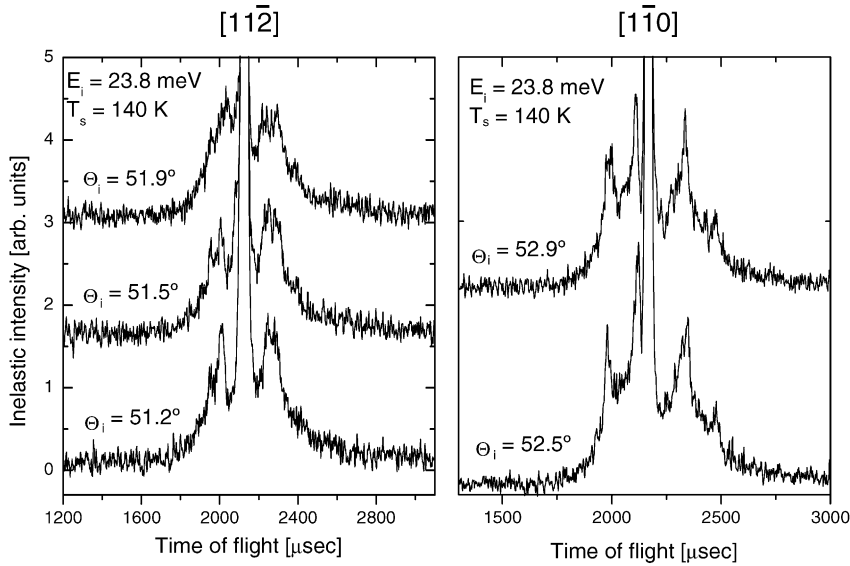


Fig. 4. TOF spectra converted into an energy-transfer scale for the  $(3 \times 3)$  phase along the two main symmetry directions. The incident momentum is  $6.75 \text{ \AA}^{-1}$  ( $E_i = 23.8 \text{ meV}$ ).

#### 4. Theoretical approach

In order to understand the origin of the phonon spectra of the  $(3 \times 3)$  reconstruction we have favored an approach that combines first-principles calculations of the phonon frequencies at the  $\bar{\Gamma}$ -point with the fitting of a second-nearest-neighbor force constant

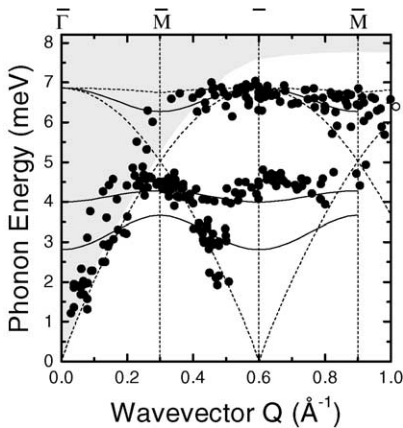


Fig. 5. Surface phonon dispersion curves for the  $(3 \times 3)$  phase. Rayleigh waves are indicated by dashed lines. Solid lines correspond to the calculated surface bands (see text). Shaded areas correspond to the projection of the  $\text{Ge}(1\ 1\ 1)$  bulk phonon modes. The surface temperature is 140 K.

model to the experimental results. This approach optimizes the use of the computationally demanding first-principles simulations: theoretical calculations at  $\bar{\Gamma}$  compensate for the lack of experimental information around that point (where the surface phonons strongly overlap with the bulk modes) and provide additional constraints to the fitting, that has to reproduce the energetic ordering and character of the modes determined in the calculations. On the other hand, the fitting is needed in order to reproduce the different phonon branches associated with the atomic vibrations normal to the surface along the main symmetry lines.

As the first step to understand the phonon dynamics of the  $(3 \times 3)$  reconstruction we have performed DFT–GGA calculations of the  $(3 \times 3)$   $\bar{\Gamma}$ -point phonon frequencies associated with the vertical ( $z$ ) displacements of the Sn atoms with respect to their positions in the ground state of the  $(3 \times 3)$  reconstruction. An effective way of calculating these three phonon frequencies, that again minimizes the computations and provides direct insight into the relevant phonon modes, is to use a modal analysis for the atomic motions. We focus on the three vibrations  $z \equiv (z_1, z_2, z_3)$ , associated with the displacement of the top most Sn atom ( $z_1$ ) and the lower Sn atoms ( $z_2, z_3$ ). These vibrations can be completely described in terms of any basis set containing three vibration modes  $\mathbf{k}_1$ ,

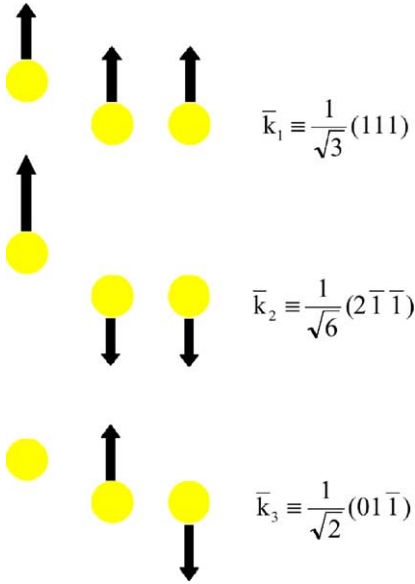


Fig. 6. Ball-and-stick model for the vibration patterns considered as a basis to describe the vertical motion of the Sn atoms.

$k_2$ ,  $k_3$  that are mutually orthogonal and normalized. The  $z$ -vibrations can be decomposed as a linear combination of the corresponding three basis vectors:  $z = \alpha k_1 + \beta k_2 + \gamma k_3$ . In our case, we have chosen as basis vectors three displacement patterns that we expect to be close to the exact phonons of the system:  $k_1 \equiv 1/\sqrt{3}(1,1,1)$ ,  $k_2 \equiv 1/\sqrt{6}(2,-1,-1)$ , and  $k_3 \equiv 1/\sqrt{2}(0,1,-1)$  (see Fig. 6). Notice that, although we refer, for the sake of simplicity, to the displacement of the Sn atoms, our calculations (both the ab initio calculations and the force constant model discussed below) involve the motion of the tetrahedra formed by the corresponding Sn atom and the three Ge atoms in the first layer bonded to it, as discussed in reference [15]. Note also that these calculations are not expected to reproduce the dispersion of the Rayleigh wave observed in the experiment.

In order to characterize the phonon modes at  $\bar{\Gamma}$ , we have to determine the dynamical matrix of the system. In our modal approach, this involves the calculation of the frequencies associated with the modes in our chosen basis set (that correspond to the diagonal elements of the dynamical matrix) and the ones associated with other displacements, that result from the mixing of these modes, in order to determine the off-diagonal (coupling) elements. Those frequencies have

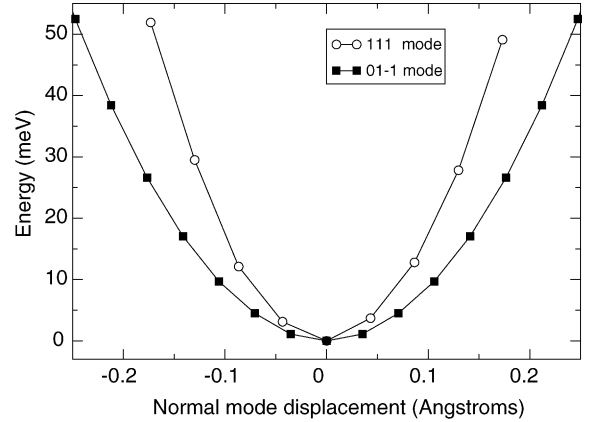


Fig. 7. Total energy curves as a function of the normal mode displacement associated with the modes  $k_1 \equiv 1/\sqrt{3}(1,1,1)$  and  $k_3 \equiv 1/\sqrt{2}(0,1,-1)$ . Notice the harmonic character of both modes. The different curvatures on the graph provide a direct comparison of the associated frequencies.

been extracted from the total energy curves as a function of the normal mode displacement  $\delta$  calculated for the following modes:  $k_1$  and  $k_3$  in our basis (see Fig. 7), as well as two other vibrations,  $(0\ 1\ 1)$  and  $(1\ 0\ 0)$ , associated with the mixing of the  $(1,1,1)$  and  $(2,-1,-1)$  modes. Notice that the  $(0,1,-1)$  represents a well-defined vibration of the  $(3 \times 3)$  reconstruction. In this calculations, the coordinates of the Sn adatoms in the  $(3 \times 3)$  reconstruction are modified according to the corresponding displacement pattern (e.g.  $\Delta z = \delta/\sqrt{3}(1,1,1)$  for the  $k_1$  mode) and kept fixed, while the rest of the atoms in the unit cell are allowed to relax to the condition of zero force in order to determine the energy of the corresponding ground state for that value of  $\delta$ .

The total energy curves have been calculated using a DFT–GGA pseudopotential method implemented in a plane wave (PW) basis set [22]. In these calculations we have used a  $(3 \times 3)$  unit-cell with six Ge atomic layers, the last one being saturated with H atoms. The technical details of the calculation are the same as in reference [15]. Cutoff and  $k$ -sampling convergence for the calculated frequencies have been thoroughly checked: errors due to these factors in the calculated frequencies are less than 0.1 meV.

Using the total energy curves in Fig. 7 we have calculated the dynamical matrix for this problem, and have obtained the phonon frequencies and character of the three vertical vibrational modes. We obtain the

following phonon energies: 5.4, 4.0 and 3.7 meV, at the  $\bar{T}$ -point of the  $(3 \times 3)$  Brillouin zone. The lowest energy corresponds to the  $(0,1,-1)$  vibration, while the two other modes are a mixture of the  $(1,1,1)$  and  $(2,-1,-1)$  modes: the highest frequency mode is mainly associated with the  $(1,1,1)$  mode, and the intermediate one with the  $(2,-1,-1)$  mode.

In parallel, we have also obtained these frequencies by fitting an up to second-nearest-neighbor coupling model to the experimental phonon frequencies. Our force constant model relates the force  $F_i$  on a given Sn adatom with its displacement (with respect to the  $3 \times 3$  structure),  $z_i$ , and the relative displacements of the surrounding adatoms,  $(z_j - z_i)$ , including effective interactions up to second nearest-neighbors:

$$F_i = -\alpha_i z_i + \sum_{j,nn} \beta_{ij}(z_j - z_i) + \sum_{k,nnn} \gamma_{ik}(z_k - z_i) \quad (1)$$

The phonon dispersion relations of the three modes, associated with the  $z$ -displacements of the three Sn atoms, are then calculated with this model and compared with the experimental results in order to determine the force constants by a least-square fit. The values that we obtained, already normalized by the corresponding atomic mass and in the proper units to get the phonon frequencies in meV, are: 58.2 (34.0) meV<sup>2</sup> for the on-site term ( $\alpha_i$ ) for the lower (upper) Sn adatom;  $-3.3$  ( $-2.6$ ) meV<sup>2</sup> for the coupling between upper and lower (lower and lower) nearest neighbor Sn adatoms; and  $-0.2$  meV<sup>2</sup> for the coupling between two second nearest neighbor Sn adatoms in lower positions. The result of the fit is shown as solid lines in Fig. 5. Our fitted model reproduces the dispersion of the three experimental modes (in the areas of the SBZ where they can be detected), and yields the following frequencies at the  $\bar{T}$ -point: 6.8, 4.0 and 2.8 meV. The fitting to the experiment and the DFT–GGA calculation yield the same energetic order and character of the modes, with values at the  $\bar{T}$ -point in reasonable agreement. In this regard, it is interesting to comment that the first principles DFT calculations (both in the LDA and GGA approximations for the exchange-correlation functional) yield a difference in energy of the  $(3 \times 3)$  reconstruction with respect to the ideal  $(\sqrt{3} \times \sqrt{3})R30^\circ$  surface of only  $\sim 4$  meV/Sn-atom. This energy difference is probably too small to explain the observed transition temperature of  $\sim 150$  K, suggesting that the frequencies calculated with the DFT–

GGA method should only be taken as a first approximation to the real spectrum at the  $\bar{T}$ -point.

In summary, the joint analysis of the DFT–GGA calculations and the fitting to the experimental data indicates that the solid lines in Fig. 5 are a good approximation to the (vertical) vibrational spectrum of the  $(3 \times 3)$  LT phase. At the  $\bar{T}$ -point, the higher band is at  $\sim 6.8$  meV, and its character is approximately  $(1,1,1)$ , while the other two bands (character at  $\bar{T}$ :  $(2,-1,-1)$  and  $(0,1,-1)$ ) appear at 4.0 and 2.8 meV.

## 5. Conclusions

High-resolution HAS has been used to study the phonon dynamics of the low temperature  $(3 \times 3)$  structure formed by 0.33 ML of Sn deposited on Ge(111). Three low-dispersion branches were observed, in addition to a Rayleigh wave. Several points corresponding to the  $(3 \times 3)$  folding of the Rayleigh wave were also observed, as expected for a well-ordered  $(3 \times 3)$  structure. We have also analyzed the phonon modes of this surface using a combination of DFT–GGA calculations and a second-nearest-neighbor force constant model. The three  $\bar{T}$ -point frequencies and the low-dispersion modes were found to be in very good agreement with experiment.

## Acknowledgements

This work has been funded by Comunidad de Madrid (contracts 07N/0022/2002 and 07N/0041/2002), the “Programa Ramón y Cajal” (Ministerio de Ciencia y Tecnología), and by the Max-Planck-Gesellschaft (Germany).

## References

- [1] B.N.J. Persson, Surf. Sci. Rep. 15 (1992) 1.
- [2] A. Mascaraque, E.G. Michel, J. Phys.: Condens. Matter 14 (2002) 6005.
- [3] J.M. Carpinelli, H.H. Weitering, M. Bartkowiak, R. Stumpf, E.W. Plummer, Phys. Rev. Lett. 79 (1997) 2859.
- [4] J. Avila, A. Mascaraque, E.G. Michel, M.C. Asensio, G. Lelay, J. Ortega, R. Perez, F. Flores, Phys. Rev. Lett. 82 (1999) 442.

- [5] O. Bunk, J.H. Zeysing, G. Falkenberg, R.L. Johnson, M. Nielsen, M.M. Nielsen, R. Feidenhans'l, Phys. Rev. Lett. 83 (1999) 2226.
- [6] A. Mascaraque, J. Avila, J. Alvarez, M.C. Asensio, S. Ferrer, E.G. Michel, Phys. Rev. Lett. 82 (1999) 2524.
- [7] J. Ortega, R. Perez, F. Flores, J. Phys.: Condens. Matter 12 (2000) L21.
- [8] T.E. Kidd, T. Miller, M.Y. Chou, T.-C. Chiang, Phys. Rev. Lett. 85 (2000) 3684.
- [9] R.I.G. Uhrberg, T. Balasubramanian, Phys. Rev. Lett. 81 (1998) 2108.
- [10] A.V. Melechko, J. Braun, H.H. Weitering, E.W. Plummer, Phys. Rev. B 61 (2000) 2235.
- [11] H.H. Weitering, J.M. Carpinelli, A.V. Melechko, J. Zhang, Science 285 (1999) 2107.
- [12] L. Petersen, et al., Phys. Rev. B 65 (2002) 020101(R).
- [13] G. Ballabio, S. Scandolo, E. Tosatti, Phys. Rev. B 61 (2000) R13345;
- G. Ballabio, S. Scandolo, E. Tosatti, Phys. Rev. Lett. 89 (2002) 126803.
- [14] L. Floreano, D. Cvetko, G. Bavdek, M. Benes, A. Morgantel, Phys. Rev. B 64 (2001) 075405.
- [15] R. Perez, J. Ortega, F. Flores, Phys. Rev. Lett. 86 (2001) 4891.
- [16] D. Fariás, W. Kaminski, J. Lobo, J. Ortega, E. Hulpke, R. Perez, F. Flores, E.G. Michel, Phys. Rev. Lett. 91 (2003) 016103.
- [17] H.J. Ernst, E. Hulpke, J.P. Toennies, Phys. Rev. B 46 (1992) 16081.
- [18] D. Fariás, G. Lange, K.H. Rieder, J.P. Toennies, Phys. Rev. B 55 (1997) 7023.
- [19] D. Fariás, K.H. Rieder, Rep. Prog. Phys. 61 (1998) 1575.
- [20] G. Comsa, Surf. Sci. 81 (1979) 57.
- [21] J. Lobo, D. Fariás, E. Hulpke, E.G. Michel, Phys. Rev. B, submitted for publication.
- [22] CASTEP 4.2 Academic version, licensed under the UKCP-MSI agreement, 1999. M.C. Payne et al., Rev. Mod. Phys. 64, 1045 (1992).